Interaction of CED-4 with CED-3 and CED-9: A Molecular Framework for Cell Death

Arul M. Chinnaiyan, Karen O'Rourke, Brian R. Lane, Vishva M. Dixit*

Previous genetic studies of the nematode *Caenorhabditis elegans* identified three important components of the cell death machinery. CED-3 and CED-4 function to kill cells, whereas CED-9 protects cells from death. Here CED-9 and its mammalian homolog Bcl-x_L (a member of the Bcl-2 family of cell death regulators) were both found to interact with and inhibit the function of CED-4. In addition, analysis revealed that CED-4 can simultaneously interact with CED-3 and its mammalian counterparts interleukin-1β–converting enzyme (ICE) and FLICE. Thus, CED-4 plays a central role in the cell death pathway, biochemically linking CED-9 and the Bcl-2 family to CED-3 and the ICE family of pro-apoptotic cysteine proteases.

The ability of an individual cell to commit suicide is essential to the overall well-being of multicellular organisms. This process, termed apoptosis, or programmed cell death, is an evolutionarily conserved, genetically regulated mechanism characterized by profound and distinct changes in cellular architecture (*1–3*). Aberrations in this process can disrupt development and homeostasis, ultimately resulting in disease (*4*). Core components of the cell death machinery have been identified with the *Caenorhabditis elegans* model system (*5*, *6*). Systematic genetic analyses have elucidated three genes, *ced-3*, *ced-4*, and *ced-9*, that are important in the regulation of nematode cell death (*7*). The CED-3 protein is an effector of cellular suicide in the nematode and is homologous to the mammalian protein ICE (also known as caspase-1) (*8*). ICE is an aspartate-specific cysteine protease of the caspase family, a subset of which function as effectors of the mammalian cell death pathway (3). CED-9, an inhibitor of cell death in the nematode, is homologous to the mammalian cell death suppressor Bcl-2 (9), the prototypic member of a growing family of cell death regulators (*10*, *11*). Whereas mammalian counterparts of CED-3 and CED-9 have been found, no mammalian homologs of CED-4 have thus far been identified. In *C. elegans*, CED-4 functions as an activator or effector of the cell death machinery (*12*, *13*).

How these components interact remains to be discovered. Epistasis analyses in the nematode suggest that *ced-9* functions genetically upstream of *ced-3* and *ced-4* (*7*, *14*). Consistent with this notion, Bcl-2 and another family member Bcl-x_L have been shown to function biochemically upstream of the caspases YAMA (CPP32; caspase-3), Mch2 (caspase-6), and ICE-LAP3 (caspase-7) (*15–17*). Ectopic expression of CED-4 in *C. elegans* neurons induces cell death that requires CED-3 activity, suggesting that CED-4 may function upstream of CED-3 (*12*). CED-4 is required for CED-9 to block apoptosis, suggesting that CED-9 may directly or indirectly regulate CED-4 activity (*12*). Here we used mammalian cells to investigate the biochemical interactions between the various *C. elegans* death proteins and some of their known mammalian counterparts. These analyses provide a simple molecular framework for the cell death machine.

CED-3 can induce cell death when expressed in mammalian cells (*18*). Similarly, ectopic expression of CED-4 in 293T human embryonic kidney cells and MCF7 breast carcinoma cells induced rapid apoptosis (Fig. 1), even though a proteolytic activity has not been ascribed to CED-4. CED-4–transfected cells displayed morphological alterations typical of cells undergoing apoptosis, becoming rounded and condensed and detaching from the dish (Fig. 1A). In MCF7 cells, CED-4 was cotransfected with the pLantern reporter construct encoding green fluorescent protein. The nuclei of cells transfected with CED-4 had an apoptotic morphology as assessed by 4′,6′-diamidino-2-phenylindole (DAPI) staining (*19*). A genetic point mutant of CED-4 (CED-4genmt; Fig. 2A), which corresponds to the mutant *ced-4* allele *n1948* (*20*), failed to induce cell death (Fig. 1B). The CED-4genmt protein was expressed in significantly lower amounts than wild-type CED-4 in 293T cells (*19*), suggesting that the isoleucine-to-asparagine (I→N) mutation at position 258 decreased the stability of the protein, which could explain the cell death–defective phenotype of *n1948* nematodes. However, another mutant of CED-4, CED-4mt, in which the two aspartic acid residues at positions 250 and 251 were altered to alanines, expressed near wild-type

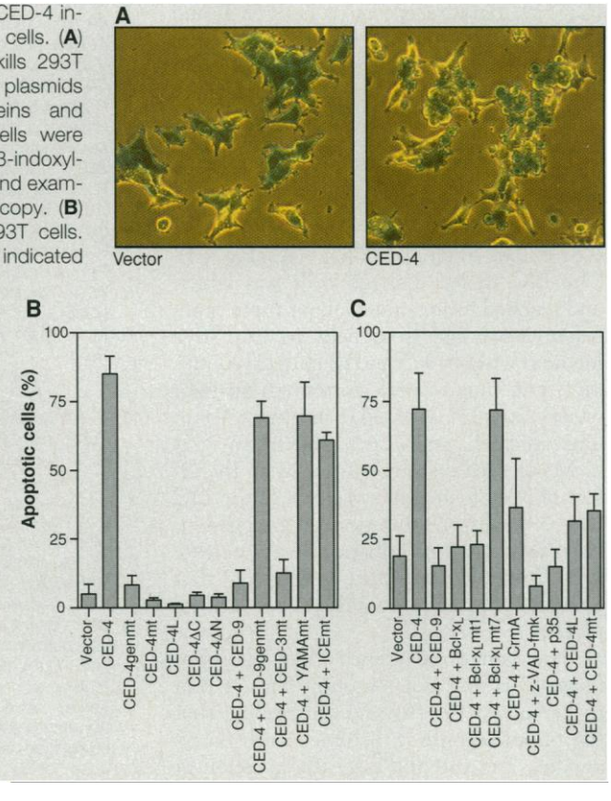

Fig. 1. *Caenorhabditis elegans* CED-4 induces apoptosis in mammalian cells. (**A**) Ectopic expression of CED-4 kills 293T cells. Cells were transfected with plasmids encoding the indicated proteins and pCMV–β-galactosidase (*30*). Cells were stained with 5-bromo-4-chloro-3-indoxyl-β-D-galactopyranoside (X-Gal) and examined by phase contrast microscopy. (**B**) Quantitation of cell death in 293T cells. Cells were transfected with the indicated expression constructs as in (A). The data (mean ± SD) are the percentage of blue cells counted that were round (with membrane blebbing) (*n* equals at least three experiments). (**C**) Quantitation of cell death in MCF7 cells. Cells were transiently transfected with the indicated expression constructs and pCMV–β-galactosidase (*30*). z-VAD-fmk was used at a 25-μM concentration. Other cell death inhibitors were used at threefold excess, and total DNA was kept constant. Cells were stained with X-Gal and examined by phase contrast microscopy (*30*). The data (mean ± SD) were analyzed as in (B).

University of Michigan Medical School, Department of Pathology, Ann Arbor, MI 48109, USA.

*To whom correspondence should be addressed.

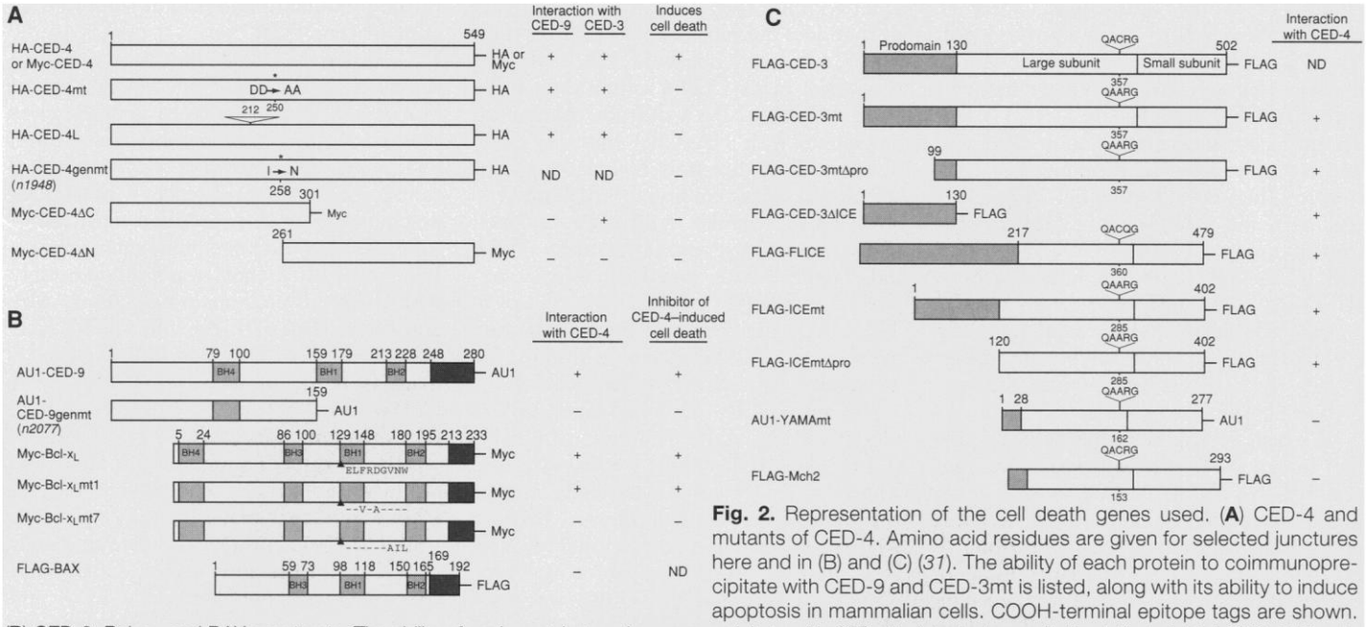

Fig. 2. Representation of the cell death genes used. (**A**) CED-4 and mutants of CED-4. Amino acid residues are given for selected junctures here and in (B) and (C) (*31*). The ability of each protein to coimmunoprecipitate with CED-9 and CED-3mt is listed, along with its ability to induce apoptosis in mammalian cells. COOH-terminal epitope tags are shown. (**B**) CED-9, Bcl-x_L, and BAX constructs. The ability of each protein to coimmunoprecipitate with CED-4 is listed, along with its ability to inhibit CED-4 killing in mammalian cells. The BH1, BH2, BH3, and BH4 domains are in gray, and the hydrophobic tail is in black. Amino acid substitutions in the BH1 domain of Bcl-x_L are shown and are previously described (*25*); dashes indicate no changes. COOH-terminal epitope tags are shown. (**C**) CED-3 and caspase constructs. The ability of each protein to coimmunoprecipitate with CED-4 is listed. The prodomain is in gray and respective active site pentapeptides shown.

amounts of protein (*19*) but also failed to induce cell death (Fig. 1B). CED-4L, which is an alternatively spliced product of the *ced-4* gene (*21*), failed to trigger cell death in the nematode as well as in mammalian cells (Fig. 1B). Instead, both CED-4L and CED-4mt functioned as dominant negative inhibitors of CED-4–induced cell death (Fig. 1C). Truncated versions of CED-4 (CED-4ΔN and CED-4ΔC, see Fig. 2A) also failed to induce apoptosis (Fig. 1B).

We next determined whether various cell death suppressors blocked CED-4–induced apoptosis. As in *C. elegans* (*12*), ectopic killing by overexpression of CED-4 in mammalian cells was blocked by CED-9 (Fig. 1, B and C). Furthermore, the CED-9 homolog Bcl-x_L abrogated CED-4 killing (Fig. 1C). Various caspase inhibitors, including CrmA, p35, and z-VAD-fmk, blocked CED-4–induced cell death, suggesting that CED-4 functions upstream of CED-3–like proteases. A mutant of CED-3 (CED-3mt) in which the catalytic cysteine is altered to an alanine abrogated CED-4 killing (Fig. 1B), consistent with the *C. elegans* data suggesting that CED-3 activity is required for CED-4 to induce apoptosis (*12*). Corresponding mutations in YAMA (YAMAmt) and ICE (ICEmt) did not significantly attenuate CED-4–induced death (Fig. 1B).

As CED-9 is a potent inhibitor of CED-4 activity in our mammalian cell system, we postulated that CED-9 may function by interacting with CED-4. To determine whether CED-4 and CED-9 interact in vivo, we transiently transfected 293T cells with plasmids that direct the synthesis of hemagglutinin (HA) epitope-tagged CED-4 and AU1 epitope-tagged CED-9. Immunoprecipitation of AU1–CED-9 quantitatively coprecipitated HA–CED-4 (Fig. 3A). Likewise, immunoprecipitation of HA–CED-4 coprecipitated AU1–CED-9 (Fig. 3A), further confirming this biochemical interaction. HA–CED-4mt and HA–CED-4L also coimmunoprecipitated with AU1–CED-9 (Fig. 3B). HA–CED-4mt is especially useful in the study of protein-protein interactions because the expression of wild-type HA–CED-4 kills cells, reducing total protein expression unless it is coexpressed with its inhibitor CED-9 (*19*). A genetic

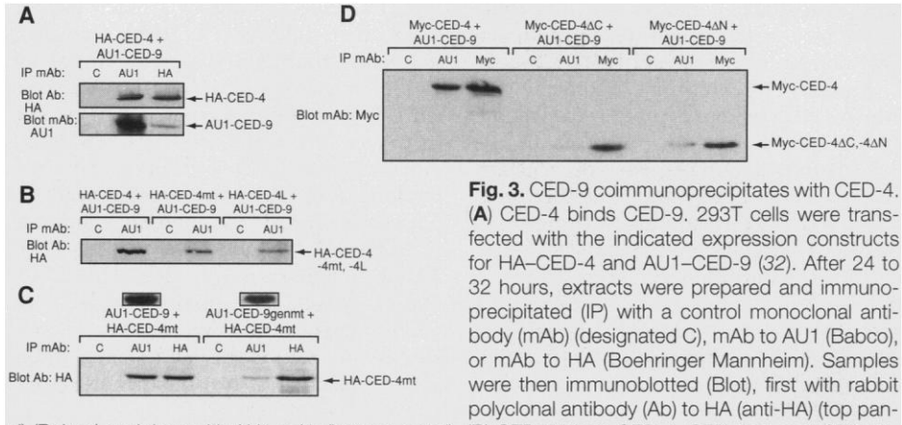

Fig. 3. CED-9 coimmunoprecipitates with CED-4. (**A**) CED-4 binds CED-9. 293T cells were transfected with the indicated expression constructs for HA–CED-4 and AU1–CED-9 (*32*). After 24 to 32 hours, extracts were prepared and immunoprecipitated (IP) with a control monoclonal antibody (mAb) (designated C), mAb to AU1 (Babco), or mAb to HA (Boehringer Mannheim). Samples were then immunoblotted (Blot), first with rabbit polyclonal antibody (Ab) to HA (anti-HA) (top panel) (Babco) and then with AU1 mAb (bottom panel). (**B**) CED-9 binds CED-4, CED-4mt, and CED-4L. Cells were transfected and lysates immunoprecipitated as in (A). Coprecipitation of HA–CED-4, HA–CED-4mt, and HA–CED-4L with AU1–CED-9 was detected by immunoblotting with anti-HA. (**C**) CED-4mt interacts with CED-9 but not CED-9genmt. Cells were transfected and lysates immunoprecipitated as in (A). Coprecipitating HA–CED-4mt was detected by immunoblotting with anti-HA. Equivalent immunoprecipitation of AU1–CED-9 and AU1–CED-9genmt are shown in upper insets. (**D**) CED-9 interacts with CED-4 but not CED-4ΔC or CED-4ΔN. Cells were transfected and lysates immunoprecipitated as in (A). For immunoprecipitation of Myc-tagged proteins, mAb to Myc (Babco) was used. Immunoblotting was done with horseradish peroxidase (HRP)–conjugated Ab to Myc (anti-Myc) (Boehringer Mannheim).

mutant of CED-9 (AU1–CED-9genmt), which corresponds to the mutant *ced-9* allele *n2077* (9), did not inhibit CED-4 killing (Fig. 1B) and did not interact effectively with HA–CED-4mt (Fig. 3C). AU1–CED-9genmt is a truncated version of CED-9 in which a stop codon is introduced at position 159 (Fig. 2B), deleting Bcl-2 homology regions 1 and 2 (BH1 and BH2). Finally, truncation of either the COOH-terminal half or the NH_2-terminal half of CED-4 (CED-4ΔC and CED-4ΔN, respectively) greatly reduced its ability to interact with CED-9 (Fig. 3D). Future studies are needed to map the domains necessary for the association of CED-4 with CED-9.

We next determined whether a mammalian homolog of CED-9, Bcl-x_L, would interact with CED-4. Analogous to CED-9, immunoprecipitation of COOH-terminal epitope-tagged Myc–Bcl-x_L coprecipitated HA–CED-4mt (Fig. 4). Similarly, immunoprecipitation of HA–CED-4mt coprecipitated Myc–Bcl-x_L (Fig. 4). An NH_2-terminal epitope-tagged version of Bcl-x_L, however, did not coprecipitate with CED-4mt (*19*), suggesting that a free NH_2-terminus is required for the biochemical interaction between Bcl-x_L and CED-4. Consistent with this, other studies emphasize the functional importance of the α-helical NH_2-terminal BH4 domain of Bcl-x_L and Bcl-2 (*22, 23*).

Mutants of Bcl-x_L (mt1 and mt15) that inhibit cell death but do not heterodimerize with a death-promoting member of the Bcl-2 family, BAX (*24*), have been identified (*25*). It was proposed that these mutants bind downstream targets (other than BAX and BAX-like proteins) that may provide insight into the mechanism by which Bcl-x_L blocks apoptosis (*25*). Consistent with their hypothesis, Myc–Bcl-$x_L$mt1 (Fig. 2B) coimmunoprecipitated with HA–CED-4mt (Fig. 4) and, in addition, blocked CED-4 killing (Fig. 1C). A mutant of Bcl-x_L that does not block cell death [Myc–Bcl-$x_L$mt7 (*25*)] did not bind HA–CED-4mt (Fig. 4) or block CED-4 killing (Fig. 1C).

FLAG-tagged BAX did not coimmunoprecipitate with HA–CED-4mt (Fig. 5A); however, BAX not only bound Bcl-x_L but attenuated Bcl-x_L binding to CED-4mt (Fig. 5, B and C). Similar results were obtained when other pro-apoptotic members of the Bcl-2 family, BAK and BIK, were co-expressed with Bcl-x_L and CED-4mt (Fig. 5C). Thus, BAX and the other death-promoting members of the Bcl-2 family disrupt the interaction between Bcl-x_L and CED-4.

Because CED-4–induced apoptosis is blocked by a catalytic mutant of CED-3 (CED-3mt) (Fig. 1B), we investigated whether CED-4 could physically engage the *C. elegans* death protease. Because wild-type CED-3 is a potent killer of 293T cells, we were unable to achieve high protein expression (*19*). Thus, we used FLAG–CED-3mt to investigate potential biochemical associations with CED-4. Immunoprecipitation analysis revealed that HA–CED-4, HA–CED-4mt, and HA–CED-4L all interacted with FLAG–CED-3mt (Fig. 6A). Myc–CED-4ΔC interacted with FLAG–CED-3mt to a much greater extent than did Myc–CED-4ΔN (Fig. 6B), suggesting that the NH_2-terminal half of CED-4 engages the apoptotic proteases. This domain alone, however, was unable to trigger cell death (Fig. 1B). To determine whether CED-4 interacts with the prodomain or "catalytic" domain of CED-3, we generated the deletion mutants FLAG–CED-3Δpro and FLAG–CED-3ΔICE, respectively (Fig. 2C). HA–CED-4mt coimmunoprecipitated with both CED-3 deletion mutants, but not FLAG-YAMA, suggesting that CED-4 may interact with CED-3 at two distinct sites, one in the prodomain and one in the protease domain (Fig. 6C).

A region of CED-4 has weak sequence similarity to the death effector domain of FLICE (*2*). CED-4–induced apoptosis was blocked by the caspase inhibitors CrmA, p35, and z-VAD-fmk (Fig. 1C), suggesting that caspases are activated by CED-4. Coprecipitation analysis revealed that CED-4 interacts with the large prodomain caspases ICE and FLICE, but nearly undetectably with the small prodomain caspases YAMA and Mch2 (Fig. 6D). As with CED-3, versions of ICE and FLICE lacking the prodomain still maintained association with CED-4 (Fig. 6D) (*19*). However, unlike CED-3mt, mutants of ICE and FLICE in which the catalytic cysteine was altered to an alanine did not effectively abrogate CED-4–induced apoptosis of 293T cells (Fig. 1B) (*19*). This may indicate that multiple caspases are activated by CED-4 and that the interaction between CED-4 and CED-3 is stronger than that between CED-4 and the mammalian caspases.

We next evaluated whether CED-4 could simultaneously bind both CED-9 and CED-3. In 293T cells, there was a weak interaction between AU1–CED-9 and FLAG–CED-3mt (Fig. 7A). However, in the presence of HA–CED-4, AU1–CED-9 was able to effectively coprecipitate with FLAG–CED-3mt, suggesting that CED-4 can biochemically link and independently interact with CED-3 and CED-9 (Fig. 7A). We postulated that a similar relation would exist between the mammalian cell death genes. Bcl-x_L did not interact well with YAMA or Mch2 in the presence or absence of CED-4mt, consistent with the inability of small-prodomain caspases to interact with CED-4. ICE and FLICE, however, interacted well with COOH-terminal epitope-tagged Myc–Bcl-x_L (Fig. 7, B and

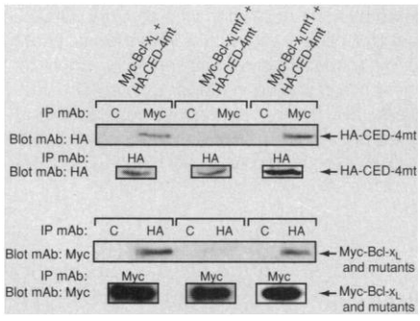

Fig. 4. Bcl-x_L associates with CED-4. 293T cells were transfected and lysates immunoprecipitated as in Fig. 3. Samples were then immunoblotted, first with anti-HA and then with HRP-conjugated anti-Myc. Smaller insets demonstrate equivalent expression and immunoprecipitation of transfectants in respective lysates.

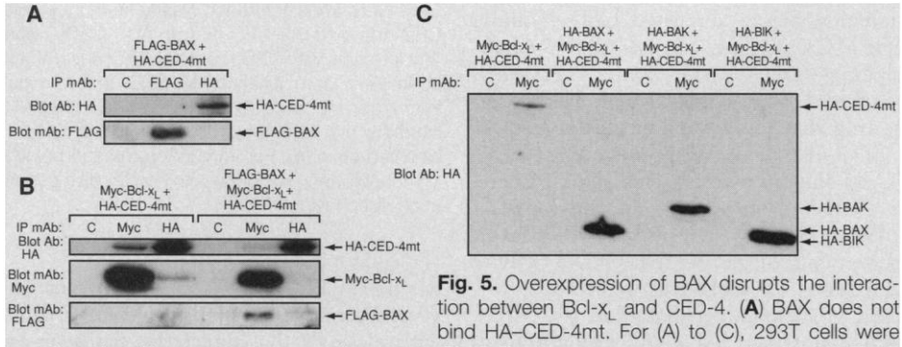

Fig. 5. Overexpression of BAX disrupts the interaction between Bcl-x_L and CED-4. (**A**) BAX does not bind HA–CED-4mt. For (A) to (C), 293T cells were transfected and lysates immunoprecipitated as in Fig. 3. For immunoprecipitation of FLAG-BAX, FLAG M2 mAb (IBI Kodak) was used. Samples were immunoblotted first with anti-HA and then with biotin-conjugated anti–FLAG M2 (IBI Kodak). (**B**) BAX disrupts the Bcl-x_L interaction with CED-4mt. Samples were sequentially probed, first with anti-HA, next with HRP-conjugated anti-Myc, and then with biotin-conjugated anti–FLAG M2. (**C**) BAX, BAK, and BIK disrupt the Bcl-x_L interaction with CED-4mt. Samples were immunoblotted with anti-HA. HA-BAX, HA-BAK, and HA-BIK are NH_2-terminal epitope-tagged and were described previously (*26*).

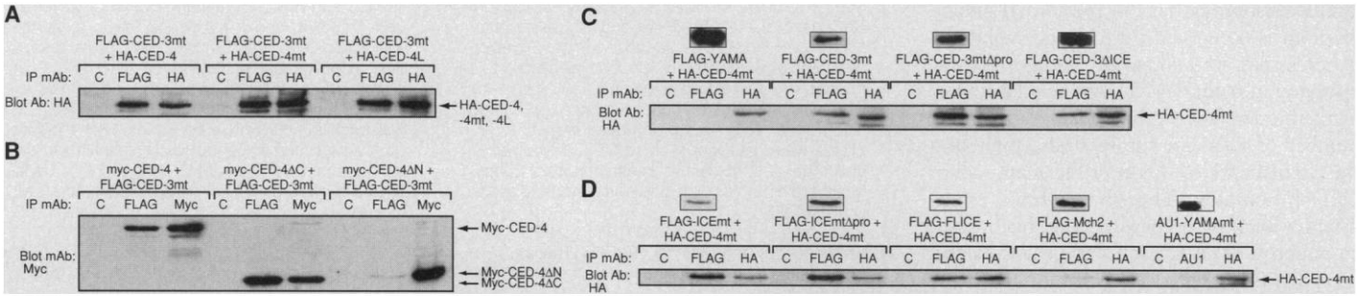

Fig. 6. CED-4 interacts with CED-3 and the caspases ICE and FLICE. 293T cells were transfected and lysates immunoprecipitated as in previous figures. (**A**) CED-3mt associates with CED-4, CED-4mt, and CED-4L. Samples were immunoblotted with anti-HA. (**B**) CED-3mt interacts with the NH_2-terminal half of CED-4. Samples were immunoblotted with HRP-conjugated anti-Myc. (**C**) CED-4mt interacts with the prodomain and the protease domain of CED-3. Samples were immunoblotted with anti-HA. Equivalent immunoprecipitation of FLAG-YAMA, FLAG–CED-3mt, FLAG–CED-3mtΔpro, and FLAG–CED-3ΔICE are shown in the upper insets. (**D**) CED-4mt interacts with ICE and FLICE but not YAMA or Mch2. Samples were immunoblotted with anti-HA. Immunoprecipitation of the various caspases are shown in the upper insets.

C), but not with NH_2-terminal–tagged Bcl-x_L or COOH-terminal–tagged BAX (*19*). FLICE did not directly bind Bcl-x_L in vitro (*19*), suggesting that the in vivo interaction between FLICE and Bcl-x_L was mediated by an endogenous protein ("factor X") expressed in 293T cells. Expression of CED-4mt did not enhance the association between ICE or FLICE and Bcl-x_L (Fig. 7B) (*19*), suggesting that endogenous factor X was sufficient and not the limiting factor to maintain this interaction. Expression of a truncated mutant of CED-4, Myc–CED-4ΔC, which binds CED-3 (Fig. 6B) but not CED-9 (Fig. 3D), significantly attenuated the ability of ICE and FLICE to coprecipitate Bcl-x_L (Fig. 7, B and C), suggesting that this mutant of CED-4 was blocking the recruitment of factor X, and thus Bcl-x_L, to the caspases tested. As predicted, expression of Myc–CED-4ΔN, which does not bind CED-3 (Fig. 6B), did not disrupt the interaction between Bcl-x_L and ICE or FLICE (Fig. 7, B and C). Finally, Myc–Bcl-$x_L$mt1 coprecipitated with FLICE, whereas the inactive Myc–Bcl-$x_L$mt7 did not (Fig. 7C), correlating with mt1 and mt7 interactions with CED-4 (Fig. 4).

Although a number of genes regulating apoptosis have been cloned and characterized, little is known about how they integrate into the molecular mechanism of cell suicide. In this study, we characterized interactions between the core components of the *C. elegans* death machinery to establish a paradigm for cell death in mammals. Previous studies have shown that Bcl-2 can partially substitute for the loss of *ced-9* function in *C. elegans* (*9*) and that CED-3 overexpression kills mammalian cells (*18*). Likewise, ectopic expression of CED-4 in mammalian cells, as in nematodes, causes apoptosis. CED-4–induced apoptosis is abrogated by CED-9, Bcl-x_L, caspase inhibitors, and a catalytic mutant of CED-3. CED-9 and Bcl-x_L interact with and inhibit the function of CED-4, which in turn can associate with and presumably activate CED-3 and the mammalian caspases.

The interaction between CED-9 and CED-4 suggests a mechanism by which Bcl-2 and Bcl-x_L block cell death. By interacting with and inhibiting CED-4 function, they abrogate its ability to activate caspases and thereby inhibit apoptosis. The death-promoting members of the Bcl-2 family, including BAX, BAK, and BIK, function by disrupting this biochemical interaction. Through an intermediary factor, Bcl-x_L associates with FLICE and ICE, thus linking the death-suppressing members of the Bcl-2 family to the pro-apoptotic cysteine proteases. A truncated derivative of CED-4 (Myc–CED-4ΔC) that interacted with CED-3 but not CED-9 attenuated the ability of Bcl-x_L to coprecipitate ICE and FLICE. A mutant of Bcl-x_L (mt1) that can block cell death and interact with CED-4 also coimmunoprecipitated with FLICE. Conversely, Bcl-$x_L$mt7, which did not block cell death or interact with CED-4, did not coprecipitate with FLICE.

In *C. elegans*, the cell death machine is relatively simple and comprises three important components: CED-3, CED-4, and CED-9. CED-4 plays a central role as a molecular death switch, interacting with and promoting the activation of the executioner protease CED-3. CED-4 is negatively regulated by direct biochemical association with CED-9, a cell death suppressor of the Bcl-2

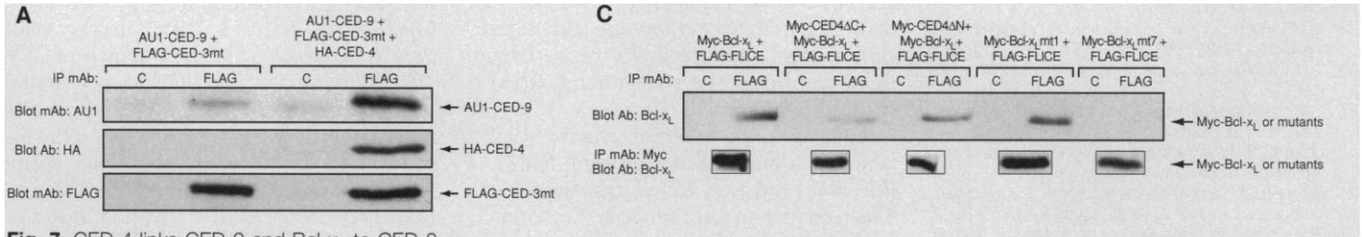

Fig. 7. CED-4 links CED-9 and Bcl-x_L to CED-3 and the caspases, respectively. 293T cells were transfected and lysates immunoprecipitated as in previous figures. (**A**) CED-3 can interact with CED-9 through CED-4. Samples were immunoblotted first with anti-HA, next with biotin-conjugated anti-FLAG M2, and then with mAb to AU1. (**B**) Coprecipitation of Bcl-x_L with ICE but not YAMA or Mch2. Samples were immunoblotted with rabbit polyclonal Ab to Bcl-x_L (Santa Cruz). (**C**) Coprecipitation of Bcl-x_L with FLICE. Samples were immunoblotted as in (B). Lower insets demonstrate equivalent immunoprecipitation of Bcl-x_L and mutants in respective lysates.

family. Assuming that this primordial suicide program is conserved throughout evolution, it holds that an analogous paradigm is recapitulated in mammals. The molecular framework that we have proposed gives rise to a number of areas for future study, including the identification of a possible mammalian CED-4 homolog. Though we have established a working framework, the mechanism by which CED-4 activates the caspases and how this is regulated by Bcl-2 family members is unknown. If a mammalian CED-4 homolog does exist, it would be a possible target for therapeutic modulation in diseases of dysregulated apoptosis.

REFERENCES AND NOTES

1. H. Steller, *Science* **267**, 1445 (1995).
2. S. Nagata, *Curr. Biol.* **6**, 1241 (1996).
3. A. M. Chinnaiyan and V. M. Dixit, *ibid.*, p. 555.
4. C. B. Thompson, *Science* **267**, 1456 (1995).
5. H. M. Ellis and H. R. Horvitz, *Cell* **44**, 817 (1986).
6. M. O. Hengartner and H. R. Horvitz, *Curr. Opin. Genet. Dev.* **4**, 581 (1994).
7. M. O. Hengartner, *ibid.* **6**, 34 (1996).
8. J. Yuan, S. Shaham, S. Ledoux, H. M. Ellis, H. R. Horvitz, *Cell* **75**, 641 (1993).
9. M. O. Hengartner and H. R. Horvitz, *ibid.* **76**, 665 (1994).
10. D. L. Vaux, *Curr. Biol.* **3**, 877 (1993).
11. E. White, *Genes Dev.* **10**, 1 (1996).
12. S. Shaham and H. R. Horvitz, *ibid.*, p. 578.
13. J. Y. Yuan, H. R. Horvitz, *Dev. Biol.* **138**, 33 (1990).
14. R. E. Ellis, J. Yuan, H. R. Horvitz, *Annu. Rev. Cell Biol.* **7**, 663 (1991).
15. A. M. Chinnaiyan *et al.*, *J. Biol. Chem.* **271**, 4573 (1996).
16. K. Orth, A. M. Chinnaiyan, M. Garg, C. J. Froelich, V. M. Dixit, *ibid.*, p. 16443.
17. R. C. Armstrong *et al.*, *ibid.*, p. 16850.
18. M. Miura, H. Zhu, R. Rotello, E. A. Hartwieg, J. Yuan, *Cell* **75**, 653 (1993).
19. A. M. Chinnaiyan, K. O' Rourke, B. R. Lane, V. M. Dixit, unpublished data.
20. J. Yuan and H. R. Horvitz, *Development* **116**, 309 (1992).
21. S. Shaham and H. R. Horwitz, *Cell* **86**, 201 (1996).
22. L. C. Lee, J. J. Hunter, A. Mujeeb, C. Turck, T. G. Parslow, *J. Biol. Chem.* **271**, 23284 (1996).
23. S. W. Muchmore *et al.*, *Nature* **381**, 335 (1996).
24. Z. N. Oltavai, C. L. Millian, S. J. Korsmeyer, *Cell* **74**, 609 (1993).
25. E. H.-Y. Cheng, B. Levine, L. H. Boise, C. B. Thompson, M. Hardwick, *Nature* **379**, 554 (1996).
26. A. M. Chinnaiyan *et al.*, *Science* **274**, 990 (1996).
27. A. M. Chinnaiyan, K. O'Rourke, M. Tewari, V. M. Dixit, *Cell* **81**, 505 (1995).
28. M. P. Boldin, T. M. Goncharov, Y. V. Goltsev, D. Wallach, *ibid.* **85**, 803 (1996).
29. A. M. Chinnaiyan *et al.*, *J. Biol. Chem.* **271**, 4961 (1996).
30. Cell death assays were done as previously described (*26–28*). Transfection of 293T and MCF7 cells was done by calcium phosphate precipitation and lipofectamine, respectively.
31. Single-letter abbreviations for the amino acid residues are as follows: A, Ala; C, Cys; D, Asp; E, Glu; F, Phe; G, Gly; H, His; I, Ile; K, Lys; L, Leu; M, Met; N, Asn; P, Pro; Q, Gln; R, Arg; S, Ser; T, Thr; V, Val; W, Trp; and Y, Tyr.
32. Expression constructs were made with pcDNA3 (Invitrogen) or pcDNA3.1(-)/MycHis (Invitrogen) and proteins epitope tagged at the COOH-terminal unless otherwise stated. Coimmunoprecipitation analyses were done essentially as described (*26, 27*). Briefly, a 50% confluent 100-mm plate of 293T cells was transfected by calcium phosphate precipitation with 5 to 10 μg of total DNA and harvested 24 to 48 hours later depending on the experiment. Cells were lysed in 1 ml of lysis buffer (50 mM Hepes, 150 mM NaCl, 1 mM EDTA, 1% NP-40, and a protease inhibitor mixture). Lysate was divided and immunoprecipitated with a control mAb or specified mAbs for 2 to 4 hours at 4°C as previously described (*29*). The beads were washed with lysis buffer (adjusted to 500 mM NaCl) three times, and precipitated immune complexes were resolved on a 12.5% SDS-polyacrylamide gel and transferred to nitrocellulose. Subsequent protein immunoblotting was performed as described (*29*).
33. J. M. Boyd *et al.*, *Oncogene* **11**, 1921 (1995).

34. Supported by the Medical Scientist Training Program (A.M.C. and B.R.L.) and NIH grant 07863 (A.M.C. and B.R.L.). We thank H. R. Horvitz for the *ced-4, ced-4L*, and *ced-3* clones, M. O. Hengartner for the *ced-9* clone and sharing unpublished data, E. Koonin for suggesting mutations in CED-4, G. Chinnadurai for the HA-BAX, HA-BAK, and HA-BIK expression constructs, and E. H.-Y.Cheng and J. M. Hardwick for the Bcl-x_L constructs. For technical help, advice, and reagents, we also thank the following members of the V.M.D. laboratory: I. Jones (preparation of figures),Y. Kuang, H. Duan, M. Muzio, J. Pan, J. McCarthy, E. Humke, T. Brtva, and C. Vincenz.

26 November 1996; accepted 22 January 1997

Interaction and Regulation of Subcellular Localization of CED-4 by CED-9

Dayang Wu, Herschel D. Wallen, Gabriel Nuñez*

The *Caenorhabditis elegans* survival gene *ced-9* regulates *ced-4* activity and inhibits cell death, but the mechanism by which this occurs is unknown. Through a genetic screen for CED-4–binding proteins, CED-9 was identified as an interacting partner of CED-4. CED-9, but not loss-of-function mutants, associated specifically with CED-4 in yeast or mammalian cells. The CED-9 protein localized primarily to intracellular membranes and the perinuclear region, whereas CED-4 was distributed in the cytosol. Expression of CED-9, but not a mutant lacking the carboxy-terminal hydrophobic domain, targeted CED-4 from the cytosol to intracellular membranes in mammalian cells. Thus, the actions of CED-4 and CED-9 are directly linked, which could provide the basis for the regulation of programmed cell death in *C. elegans*.

Programmed cell death (PCD) plays an essential role in animal development and homeostasis (*1*). Genetic studies in the nematode *Caenorhabditis elegans* have identified several components of the death pathway, some of which are conserved in vertebrates, including humans (*2, 3*). The nematode *ced-9* gene was discovered by analysis of gain-of-function mutants, and it was subsequently shown that *ced-9* protects cells that normally survive from undergoing PCD (*4*). In contrast, loss-of-function mutations in the *ced-3* gene cause all 131 cells that normally die to survive, indicating that *ced-3* is required for PCD (*3*). Both *ced-9* and *ced-3* have mammalian homologs. The *ced-9* gene encodes a protein with significant sequence homology to the vertebrate Bcl-2 and Bcl-x_L survival proteins, whereas the *ced-3* product is homologous to the interleukin-1β–converting enzyme (ICE), which is a member of a growing family of ICE-like proteases, called caspases (*5, 6*). The mammalian *bcl-2* gene can functionally substitute for *ced-9* in *C. elegans* (*5, 7*), suggesting that Bcl-2 is a mammalian homolog of CED-9. Another *C. elegans* gene, *ced-4*, is required for developmental cell death in the worm, and its overexpression can cause cells that normally survive to undergo PCD (*8, 9*). Genetic experiments have indicated that *ced-9* controls cell death by preventing the activation of the death genes *ced-3* and *ced-4* (*4, 9*) and have suggested that *ced-3* acts downstream of *ced-4* and that *ced-9* acts upstream of *ced-4* (*4, 9*). Consistent with this, Bcl-2 and Bcl-x_L can inhibit the activation of ICE-like proteases and therefore appear to function upstream of the death proteases in the mammalian apoptotic pathway (*10*).

To search for proteins that bind to CED-4, we screened a *C. elegans* cDNA library for CED-4–interacting proteins by using GAL4–CED-4S as a "bait" in the yeast two-hybrid assay (*11*). In a screen of 2×10^6 library clones, four cDNAs were found to interact with the GAL4–CED-4 but not with control baits. One of the CED-4–interacting cDNAs encoded the entire CED-9 coding region fused in-frame to the GAL4 transcriptional activation domain. The association of CED-4 with CED-9 was specific in that CED-4 was unable to interact with empty vector or several plasmids encoding irrelevant baits (Fig. 1A) (*12*). To further characterize the CED-4–CED-9 interaction, we determined the ability of CED-4 to associate with three natural CED-9 mutants (Fig. 1A). In the yeast two-hybrid system, CED-4 interacted with the

Department of Pathology and Comprehensive Cancer Center, The University of Michigan Medical School, Ann Arbor, MI 48109, USA.

*To whom correspondence should be addressed. E-mail: gabriel.nunez@umich.edu